

## INDUSTRIAL PERSPECTIVE ON FOULING RESEARCH - FOULING MITIGATION THROUGH MODIFICATIONS OF HEAT TRANSFER SURFACES

L. Jackowski<sup>1</sup>, T.Y. Lam<sup>2</sup>, E. Rogel<sup>1</sup>, C. A. Bennett<sup>3</sup>, K. Hench<sup>1</sup>, S. Taylor<sup>1</sup>, and T. Swangphol<sup>4</sup>

<sup>1</sup> Chevron Energy Technology Company, Richmond, CA, USA, [ljau@chevron.com](mailto:ljau@chevron.com)

<sup>2</sup> Chevron Global Downstream, El Segundo, CA, USA

<sup>3</sup> Chevron Energy Technology Company, Houston, TX, USA

<sup>4</sup> Chevron Technology Ventures, Houston, TX, USA

### ABSTRACT

Most academic research activities on heat exchanger fouling in refineries are focused on the crude unit preheat trains, especially the hottest heat exchangers. Predictive models that have been proposed to describe fouling behavior in heat exchangers typically include fitting parameters established from either laboratory experiments or field data. Despite decades of research there is limited progress in developing design guidelines leading to significant reduction in heat exchanger fouling rates. This paper discusses the inability to duplicate field conditions in laboratory scale experiments. Detailed chemical analysis shows that fouling deposits formed in operating heat exchangers contain mainly inorganic material bonded by heavy hydrocarbons while fouling deposits collected in laboratory scale experiments contain mainly hydrocarbons. Consequently, one would expect different threshold conditions for fouling in the laboratory environment versus the operating plants. Furthermore, fouling resistances predicted from routine heat exchanger monitoring could be misleading and result in erroneous fitting parameters in the predictive fouling models.

This paper describes experimental techniques for analyzing fouling mitigation technologies involving modifications of the heat transfer surfaces.

### INTRODUCTION

Fouling of heat exchangers in the refining industry results in significant economic penalties. Detailed studies performed by Van Nostrand et. al. (1981) for a hypothetical refinery processing 100,000 barrels (15,900 cubic meters) of crude oil per day estimated total cost of fouling of nearly 10 million US dollars. Applying a cost escalation factor of 2.73 and extrapolating the crude oil refining capacity to 75 million barrels per day (corresponding to current global refining throughput), the worldwide cost of fouling is about 20 billion US dollars per year (2016 prices). As noted in that paper, the estimates were conservative by including only fouling related expenses comprising of additional energy cost, loss of production, maintenance and cleaning for major refinery units and excluding cost of fouling for miscellaneous operations such as power generation and cooling of process streams with water and air cooled heat exchangers.

In addition to economic and environmental impact manifested through higher CO<sub>2</sub> emissions, fouling in refinery heat exchangers may lead to inducing unexpected damage mechanisms such as high temperature hydrogen attack and high temperature sulfidation corrosion (Jackowski et. al., 2017). Consequently, fouling in the refinery heat exchangers is also a safety and plant integrity issue.

Wilson et. al., (2015) summarized research on fouling in heat exchangers processing crude oil in three categories: deterministic models, threshold models, and artificial neural network approaches. In addition, Bennett (2012) proposed a threshold model describing asphaltene fouling derived from fundamental analysis of adhesion forces and shear stress. Bennett (2016) also proposed a fundamental threshold model for the sedimentation particulate fouling mechanism.

In this paper, we compare fouling deposits collected from operating heat exchangers and fouling deposits created in laboratory experiments using the same crude oil. Significant differences in chemical composition and physical characteristics of fouling deposits indicates that neither laboratory experiments nor fundamental fouling analyses relate closely to conditions experienced in the industrial environment.

Another approach to develop predictive fouling models is analysis of trend data of the operating heat exchangers or heat exchanger networks to derive constant parameters in the assumed model (Pugh and Ishiyama, 2015). This method works well for consistent sets of field data and for exchangers where fouling resistance on the crude side is dominant. This paper illustrates difficulties in the analysis of fouling trend data and possible scenarios leading to false fouling trends.

Instead of developing new improved fouling models, we present an alternative approach to fouling research that focuses on simplified experiments to evaluate fouling mitigation techniques that involve modifications of heat transfer surfaces.

## COMPARISON OF FOULING DEPOSITS OBTAINED IN LABORATORY EXPERIMENTS AND REFINERY HEAT EXCHANGERS

Laboratory fouling experiments are often carried out to predict fouling propensity of various crude slates (Smith, 2013, Bennett et. al., 2009) and developing threshold fouling models such as that by Ebert and Panchal (1997). Our observations of actual heat exchangers in industrial facilities indicate significant differences between the fouling threshold observed in the field and those determined by laboratory experiments. To illustrate possible causes of these discrepancies we analyzed fouling deposit samples collected from actual heat exchangers from two refineries and the fouling deposit samples obtained in the laboratory once-through test rig using the corresponding feeds.

Table 1. Comparison of operating conditions in refinery heat exchangers and laboratory tests.

	Exchanger in Refinery A	Exchanger in Refinery B	Lab
Preheat Train Location	Downstream of Flash Drum	Upstream of Desalter	NA
Stream Allocation	Tube Side	Shell Side	Annulus
Max. Temp. <sup>1</sup> °C	310	200	380
Shear Stress <sup>2</sup> , Pa	8-15	0.5 – 5 <sup>4</sup>	nil
Tube Material	316 Stainless Steel	Carbon Steel	316 Stainless Steel
Deposition Time <sup>3</sup>	3 years	1 year	1.5 day

<sup>1</sup> Maximum wall temperature in the heat exchanger and lab experiment at the sample collection point.

<sup>2</sup> Shear stress calculated at clean conditions

<sup>3</sup> Deposition time corresponds to time interval from start at clean conditions to turnaround at which time the deposit samples were collected

<sup>4</sup> Shell side shear stresses were calculated using the HTRI software, whose methods are very similar to those recently published by Bennett and Hohmann, 2017

As shown in Table 1, the deposition time interval varies significantly between the actual heat exchangers and the laboratory experiments. Naturally, this difference is unavoidable due to practical limitations. In addition, the laboratory experiments were carried out at higher tube wall temperatures than those observed in the field heat exchangers. This was done in order to accelerate fouling. For the same reason, shear stress in the laboratory tests was nearly zero to eliminate fouling removal/suppression.

It should be added that the experiments carried by Ebert and Panchal (1997) leading to the first threshold model were also carried out at elevated temperatures corresponding to coking conditions.

### Sample Analysis

Deposits from heat exchangers A and B described in Table 1 were ground to ensure proper homogenization of the samples. Soluble hydrocarbon components were extracted from deposits using a Soxhlet apparatus (Kuo and Mitra,

2003). After extraction, the solvent was evaporated to recover the hydrocarbon components. The remaining solid was dried under nitrogen. After drying the samples, insoluble materials were analyzed to determine mineral phases and coke presence. Soluble hydrocarbon materials were analyzed to determine asphaltene solubility distribution and asphaltene content. Mass balances for the extractions were in the 90-110% range (i.e. within the experimental error of the separation Soxhlet technique).

Deposits from fouling tests were scraped from tubes and sent directly for elemental and infrared analyses. Extraction of soluble components was also carried out.

### Characterization Methods

**X-Ray Diffraction (XRD).** The sample was ground and mounted on a sample holder. In these tests, X-rays were directed at the sample, and the diffracted rays were collected. The intensity of diffracted X-rays was continuously recorded as the sample and detector were rotated through their respective angles. Diffraction patterns were used to identify mineral phases.

**Elemental Analysis.** Elemental analysis was carried out using a Thermo Scientific Flash 2000. In these tests, the sample was combusted and the combustion products were separated and quantitatively determined with a thermal conductivity detector.

**Asphaltene concentrations and asphaltene solubility profile.** Asphaltene concentrations and asphaltene solubility profiles were determined using on-column filtration techniques (Rogel et al., 2009, Rogel et al., 2010). In these techniques, a solution of the sample is injected into a column packed with an inert material using n-heptane as the mobile phase. This solvent induces the precipitation of asphaltenes and, as a consequence, their retention in the column. To determine the asphaltene content the mobile phase is switched to a blend dichloromethane/methanol 90/10 v/v that re-dissolves the asphaltenes completely. Asphaltenes are quantified using an Evaporative Light Scattering Detector (ELSD). This technique produces results that correlate with the results obtained using the conventional gravimetric technique, ASTM 6560 (ASTM, 2005).

In the asphaltene solubility profile technique, after the initial injection and precipitation of asphaltenes, the mobile phase is changed gradually from pure n-heptane to 90/10 methylene chloride/methanol and then to 100 % methanol. This procedure gradually re-dissolves the asphaltenes from the easy to dissolve (low solubility parameter) to the hard to dissolve (high solubility parameter) producing a distribution that represents the range of asphaltenic species with different solubilities.

**Infrared Spectra.** Infrared spectra were obtained in a Varian 7000e FT-IR infrared spectrophotometer. Transmission measurements were carried out on a Diamond Anvil Cell (DAC), which is used to compress the sample for transmission analysis. Spectra were measured from 4000cm<sup>-1</sup> to approximately 400 cm<sup>-1</sup> using a Deuterated Triglycine Sulfate (DTGS) detector as the average of 32 scans acquired at 4 cm<sup>-1</sup>.

## Results and Discussion

Table 2 shows properties of the two crude oils and a comparison of the main characteristics of the deposits obtained from the heat exchangers and fouling tests. In this table, mineral compositions of the insoluble material are also reported as well as the carbon and hydrogen content of the deposits. It is important to mention that only major mineral components are listed. Minor or trace components were omitted. These results showing the mineral composition indicate a complex deposition mechanism that obviously occurs during extended periods of time. As expected, this is not observed in the fouling bench tests. In particular, the formation of oxides and sulfides, as well as the accumulation of other minerals requires longer time scales as these

processes need foulants that are in small concentrations in the crude oil that is fed to heat exchangers. Additional to the presence of minerals, the content of hydrogen and carbon is related to the nature of the organics present in the deposit. Unfortunately, the amount of deposit A recovered after the fouling test was insufficient to evaluate hydrogen and carbon content. However, for deposit B, the molar hydrogen to carbon ratio is lower for the one obtained from the exchanger (1.19) than for the one coming from the fouling experiment (1.36) indicating that the first one is more aromatic. Additionally, the table shows that exchanger deposits contain soluble components while laboratory fouling deposits lack them.

Table 2. Comparison of deposits from the same feed and different sources: Refinery Exchanger and Laboratory Test Rig.

Samples	Percentage of Insoluble Components (wt. %) <sup>1</sup>	Major Mineral Components	Carbon (wt. %)	Hydrogen (wt. %)	Molar Hydrogen/Carbon Ratio
Refinery A Crude Feed	32.9 °API, 1.96 wt. % Sulfur, 986 ppm Nitrogen, Viscosity at 40°C: 5.85 cSt				
Exchanger in Refinery A	83	Pyrite FeS <sub>2</sub> Silicon Oxide SiO <sub>2</sub>	40.29	2.66	0.79
Laboratory test with the same feed as in Refinery A	100	None	N.D <sup>2</sup>	N.D <sup>2</sup>	N.D <sup>2</sup>
Refinery B Crude Feed	39.5 °API, 0.476 wt. % Sulfur, 968 ppm Nitrogen, Viscosity at 40°C: 2.89 cSt				
Exchanger in Refinery B	34	Pyrite, FeS <sub>2</sub> Greigite, Fe <sub>3</sub> S <sub>4</sub> Iron Sulfide, FeS Magnetite, Fe <sub>3</sub> O <sub>4</sub> Magnesium Oxide MgO Sodium Chloride NaCl	64.78	6.43	1.19
Laboratory test with the same feed as in Refinery B	98	None	76.08	8.61	1.36

<sup>1</sup> Insoluble in Methylene Chloride (CH<sub>2</sub>Cl<sub>2</sub>)

<sup>2</sup> N.D: Not enough deposit to determine carbon and hydrogen.

The analysis of the soluble components of the exchanger deposits shown in Table 3 indicates that they have relatively higher amounts of asphaltenes in comparison with the feeds. These larger amounts indicate the enrichment of these refinery deposits in the heaviest components in the crude oil. In contrast to the asphaltene contents of the refinery deposits, fouling test deposits do not have asphaltenes. Additionally, comparisons of solubility profiles of organic extracts with their own feed oils (see Figures 1 and 2 for exchangers A and B, respectively) reveal that the organic extracts contain asphaltenes that are less soluble than those present in the feed oils. This behavior can be inferred by the displacement of the second asphaltene peak in the organic extracts relative to the same peak in feed A. In the particular case of feed B, solubility profile of deposit refinery B shows a second peak that it is not present in the feed.

Table 3. Asphaltene content of the soluble components

Sample	Asphaltene Content (wt. %)
Feed A	2.0
Exchanger A	10.4
Fouling Test A	0.0
Feed B	1.2
Exchanger B	3.8
Fouling Test B	<<1.0

The displacement towards higher times is normally observed for processed samples. Cracking and coking reactions that eliminate alkyl chains and increase the aromatic condensation degree of asphaltenes are responsible for the lower solubility of these asphaltenes and the shifting of the second peak to the right of the chromatogram (Lopez-

Linares et al., 2011, Rogel et al., 2013). This could be evidence that the material in the deposit reacted to produce these changes in the asphaltenes. Also, for thermodynamic reasons, asphaltene molecules with lower solubility are preferentially precipitated to form deposits. Similar results indicating the enrichment of deposits in the least soluble asphaltenes has been reported before for deposits from refineries (Rogel et al., 2014) as well as from the oilfield (Rogel et al., 2015)

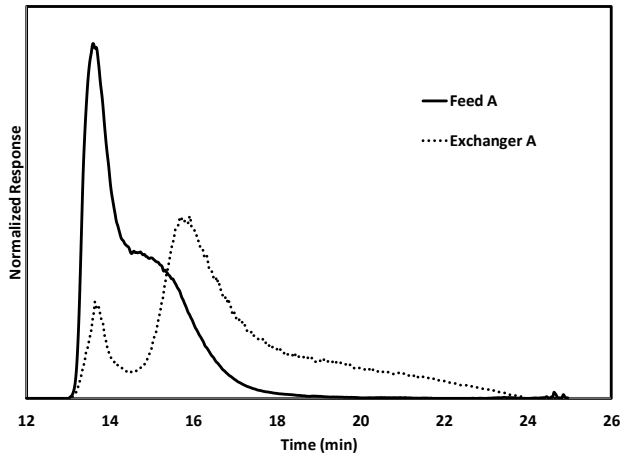


Figure 1. Comparison of asphaltene solubility profiles of feed A and its exchanger deposit.

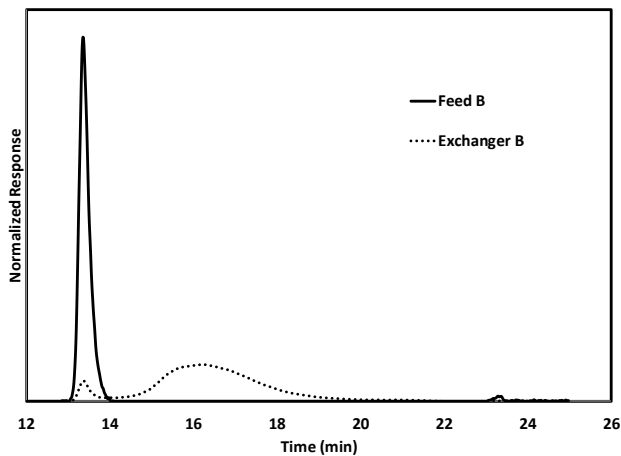


Figure 2. Comparison of asphaltene solubility profiles of feed B and its exchanger deposit.

FTIR was used to analyze the deposits. In this technique, the absorbance of the molecule in the infrared spectrum is associated with its molecular structure. Different functional groups produce different characteristics bands. For instance, the presence of aliphatic chains is associated with a band around  $2920\text{ cm}^{-1}$  that corresponds to the stretching of the C-H bonds in aliphatic chains. Also, it is known that the presence of carbonaceous material is associated to a shift in the baseline of the spectrum.

Figure 3 shows a comparison of the FTIR spectra of the fouling deposits A and B. This comparison indicates a remarkable similarity. A quantitative way to evaluate the relative content of the carbonaceous residual material is to measure the signal at  $2000\text{ cm}^{-1}$  where there are no other

spectral features relative to the signal at  $2920\text{ cm}^{-1}$  (-C-H stretching) ( $2000\text{ cm}^{-1}/2920\text{ cm}^{-1}$  ratio). The calculated ratios (0.66 vs. 0.62 for the exchanger deposit) indicate that these deposits have approximately similar contents of carbonaceous insoluble residue. This is also an indication of similar hydrogen deficiencies that could not be compared directly because of the lack of elemental analysis for the fouling deposit A. In agreement with this finding, both deposits have small signals at  $2920\text{ cm}^{-1}$  for the -C-H stretching indicating the disappearance of aliphatic chains due to cracking reactions during the fouling process.

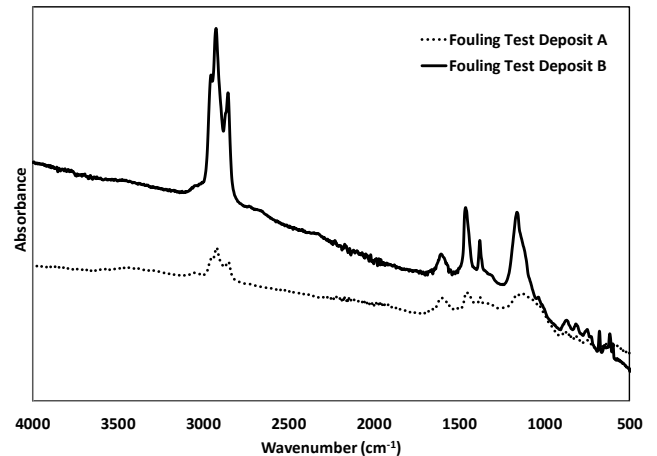


Figure 3. FTIR spectra for fouling deposits obtained from Feeds A and B

The comparison of deposits B is presented in Figure 4. In this case, only the deposit B from the fouling test showed a significant shift due to carbonization processes. In fact,  $2000\text{ cm}^{-1}/2920\text{ cm}^{-1}$  ratio is lower for the exchanger deposit (0.21) than for the fouling test deposit (0.37). However, other features like the relative signals around  $2900\text{ cm}^{-1}$  and  $1500\text{ cm}^{-1}$  are similar.

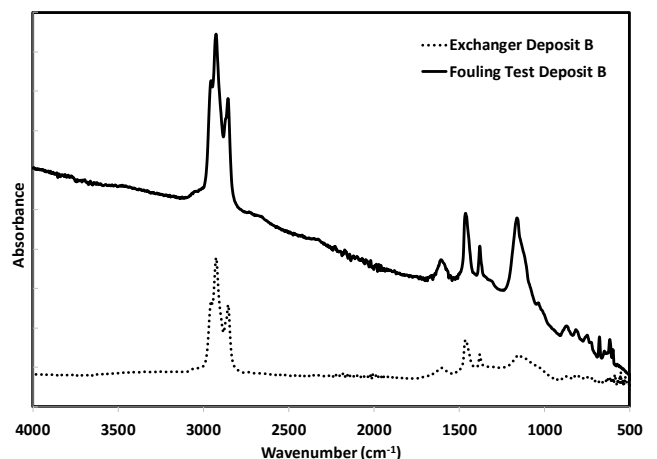


Figure 4. FTIR spectra for deposits obtained from Feed B

To evaluate in more detail differences in the deposits, the elemental analysis of the exchanger deposits after the extraction of soluble components was carried out. The results are shown in Table 4. In this table, it is clear that the insoluble residue in exchanger deposit A is highly deficient in

hydrogen with a molar H/C ratio of 0.57 indicating cracking and possible condensation reactions that lead to coke formation. On the contrary, the carbonaceous residue in exchanger deposit B shows a comparatively high molar H/C ratio (1.04), similar to the one found for heavy hydrocarbons, which is consistent with the small shift observed in its IR spectrum (Figure 4). These results are in agreement with the operational maximum temperatures of the heat exchangers (see Table 1) that indicates that exchanger A is closer to the coking temperature region.

Table 4. Elemental analysis of insoluble components of Exchanger Deposits.

Sample	Carbon (wt. %)	Hydrogen (wt. %)	Molar H/C Ratio
Exchanger A	33.69	1.61	0.57
Exchanger B	65.03	5.62	1.04

In summary, there are significant differences between the deposits obtained in the laboratory using accelerated fouling tests and those coming from the preheat train heat exchangers. For this reason, one could expect that fouling threshold models determined based on the laboratory experiments could differ from the threshold fouling conditions observed in the operating plants.

#### ANALYSIS OF FOULING MONITORING DATA FOR SELECTED CRUDE PREHEAT EXCHAGERS

Within the industry, critical heat exchangers are monitored for fouling and thermal performance to predict future maintenance activities such as cleaning and repairs. In general, the heat exchanger monitoring relies on comparison between the actual thermal performance and that predicted from a heat exchanger simulator at the same process conditions but with absence of any fouling. The fouling resistance is calculated according to the following formula:

$$R_f = 1/U_{observed} - 1/U_{clean} \quad (1)$$

Where:

$$U_{observed} = Q/(A MTD) - \text{based on field data} \quad (2)$$

$$U_{clean} - \text{calculated with an exchanger simulator} \quad (3)$$

The exchanger heat duty  $Q$  is calculated based upon heat capacity and field measurements of flow rates and inlet/outlet temperatures. Overall heat transfer coefficient  $U_{clean}$  is calculated by using a single heat exchanger simulator or a simulator of the heat exchanger network assuming clean conditions. In some heat exchanger network simulators (Pugh and Ishiyama, 2015) trend data obtained from the heat exchanger network are being used to calculate fitting parameters in a chosen fouling model such as Ebert and Panchal (1997) or Polley (2010), for example.

To illustrate common difficulties in monitoring the heat exchangers, we are presenting three examples of fouling trends for the heat exchangers operating in Refinery C preheat train. As described in Table 5, the exchanger E-1 operates in the cold section of the preheat train, the exchanger E-2 is located just downstream of the flash drum and the exchanger E-3 is the hottest exchanger in the network placed just upstream of the atmospheric column furnace.

Table 5. Operating conditions of the monitored heat exchangers in the Refinery C crude preheat train.

Exchanger	E-1	E-2	E-3
Preheat Train Location	Upstream of Desalter	Downstream of Flash Drum	Downstream of Flash Drum
Tube Side	Raw Crude	Flashed Crude	Flashed Crude
Shell Side	Jet	LVGO	Vac. Resid.
Tube wall Temp. Range (°C)	100-150	170-200	290-300
Tube Wall Material	Carbon Steel	Carbon Steel	Stainless Steel
Tube Side Shear Stress Range (Pa)	6-8	6-9	10-15

Fouling resistance of the heat exchanger E-1, see Figure 5, shows a behavior that could be interpreted as either linear or asymptotic. If we stopped the exchanger monitoring in September 2015 we would describe this fouling behavior as linear. Alternatively, if we stopped the exchanger monitoring in May 2016 we would describe the fouling behavior as asymptotic. For the given tube wall temperatures and shear stress we do not expect any significant fouling on the crude side. Therefore, we expect that much of the fouling takes place in the shell side (jet fuel). This conclusion needs to be confirmed during the next turnaround.

Nearly zero fouling for the exchanger E-2, see Figure 6, conforms to our expectations while the fouling trend for the heat exchanger E-3, shown in Figure 7, is almost impossible to explain. Rapid increases and decreases of fouling resistance imply frequent cleaning. However, during nearly three years of operation, this heat exchanger has never been taken out of service. Trying to explain this unusual fouling resistance trend we considered the following possible scenarios:

- Vacuum residuum stream may contain coke particles that accumulate on the shell side and are being pushed out once there is enough pressure drop buildup
- Changes in vacuum residuum transport properties result in changes in shell side heat transfer coefficients that are not properly captured by the heat exchanger simulator. The simulator used was HTRI Xist software which requires geometry, process, and transport properties definition.
- Shell side flow regime changes between laminar and turbulent are not properly represented by the heat exchanger simulator.

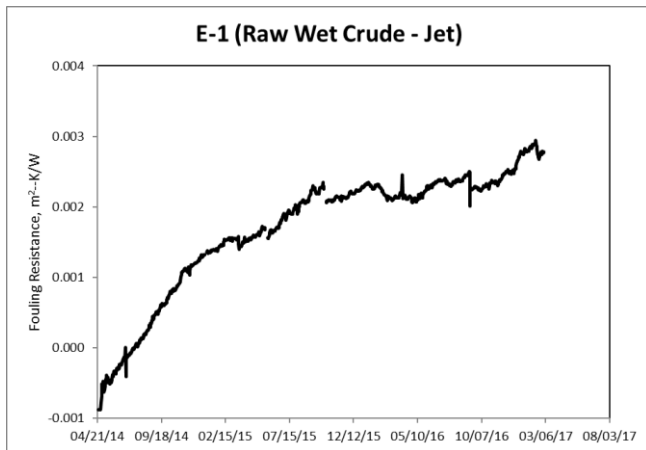


Figure 5. Trend of fouling resistance trend in a heat exchanger upstream of a desalter.

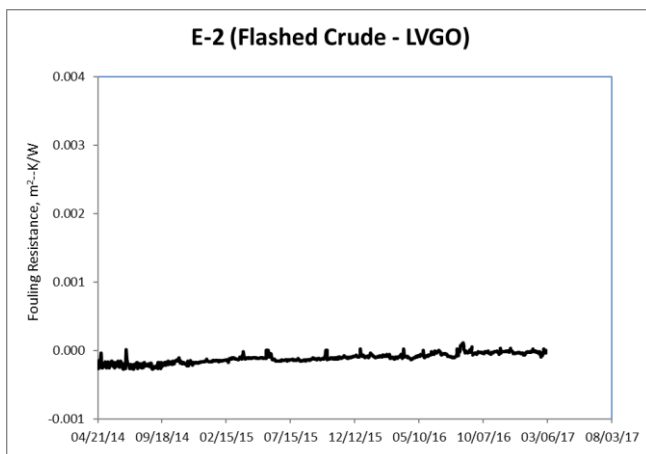


Figure 6. Trend of fouling resistance in a heat exchanger downstream of a flash drum.

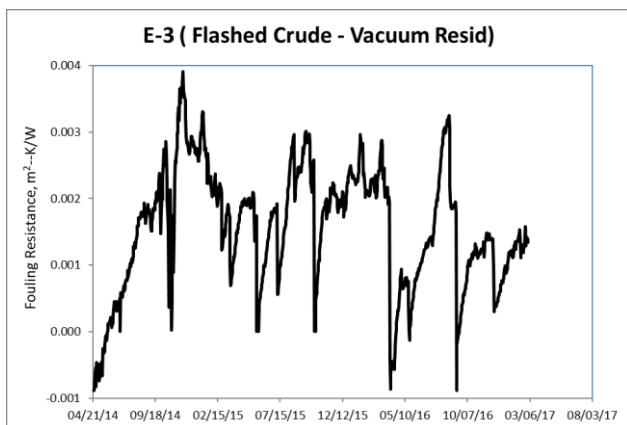


Figure 7. Trend of fouling resistance in a hottest heat exchanger downstream of a flash drum, just upstream of the atmospheric furnace.

It should be noted that during the quest to determine the threshold fouling conditions or predictive fouling models we focus on the crude side while likely explanations of fouling trends focus on the other streams. Consequently, analysis of

trend data alone could lead to inaccurate predictions of fitting parameters in the fouling models.

#### LABORATORY APPARATUS TO STUDY FOULING MITIGATION TECHNOLOGIES THROUGH MODIFICATIONS OF HEAT TRANSFER SURFACE

The fouling process is often described as a difference between deposition and removal, Eq. 4.

$$dRf/dt = \{Deposition\} - \{Removal\} \quad (4)$$

Wilson et al. (2015) compiled several fouling models devolved over the years of research. In all models, deposition is a strong function of surface or film temperature, velocity and fluid transport properties while the removal term, often called the suppression term, is a strong function of shear stress at the heat transfer surface. Following this understanding, we focused on heat transfer surface modifications that will make the removal term large enough to limit the rate of fouling. One of the ways to enhance the removal term is reduction of the adhesion forces between fouling deposits and the heat transfer surface through application of low surface energy coatings that are repellant to common process fluids such as crude oil and water.

As mentioned before, the laboratory experiments cannot replicate actual field conditions just by maintaining the same fluid velocities and surface temperatures. The time scale, impurities, ever-changing crude slates, and once through operation is about impossible to accomplish using laboratory scale conditions. For this reason, our laboratory work focused on development of fouling mitigation technologies as opposed to development of new and improved fouling models. Having said that, the authors recognize that laboratory experiments yield valuable information on fundamental physical and chemical mechanisms.

In order to accelerate fouling rates, the base experiments are carried out at very low, 5-10 mm/s, velocities that result in about zero shear stress at the heat transfer surface. Once the deposit is formed, fluid flow rate may be increased to accomplish shear stress conditions that are similar to those experienced in the operating heat exchangers. This concept is shown schematically in Figure 8. Process fluid flows in the annular space between outer stationary tube and the inner removable tube. A cartridge heater installed inside the inner tube provides necessary heat input to maintain a desired heat transfer surface temperature. Such an arrangement allows for easy access to the heat transfer surface and collection of fouling deposits.

An example of the test results is shown in Figure 9. At nearly zero shear stress conditions and tube wall temperature of 205 °C, fouling resistance for bare carbon steel tube started rising continuously after about 30 hours. For the coated tube, fouling resistance started rising at somewhat lower rates after about 90 hours. To verify weak adhesion between fouling deposit and coated tube, the process flow was increased to develop shear stress at the inner tube wall of about 12 Pa. Following the high shear stress operation, fouling resistance dropped to about zero implying that all deposit has been removed. Visual inspection of the coated tube confirmed this conclusion. It was also confirmed via visual inspection that

fouling deposit adhered strongly to the bare uncoated surface. For this reason, the high shear stress test was not carried out for the bare carbon steel tube.

The cost of evaluated coating technologies varies from 20 to 80% of the tube bundle cost depending on the tube bundle size and material. At this moment, there is not enough information about longevity of new anti-fouling coating technologies. To make these fouling mitigation technologies commercially attractive on a wide scale in the oil and gas industry, a coating life of 10 years, corresponding to two turanarounds in a typical operating unit, is needed.

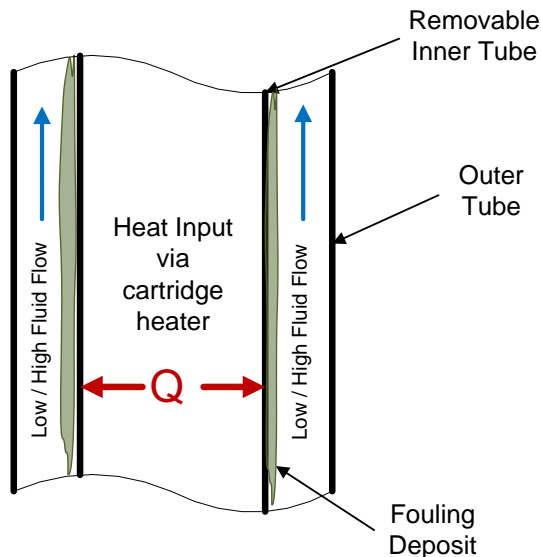


Figure 8. Schematics of the test apparatus to study impact of coatings on fouling rates.

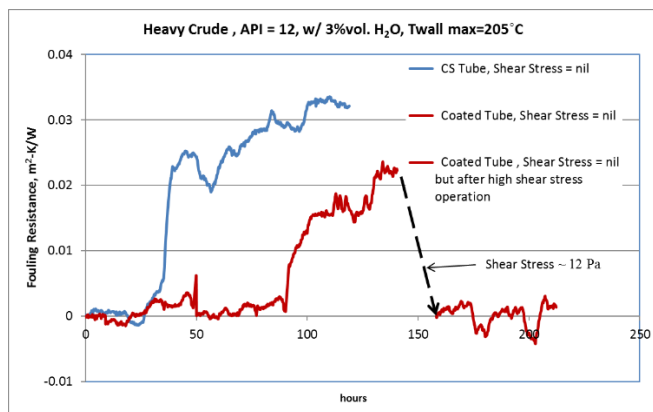


Figure 9. Experimental results showing fouling resistance for two cases, a bare carbon steel tube and a coated tube.

The annular experiments illustrated in Figures 8 and 9 require significant extrapolations to field conditions. Uncertainties related to this extrapolation can be reduced by performing fouling tests in a small-scale heat exchanger shown in Figure 10. This test heat exchanger contains a symmetrical two-pass tube layout with respect to the vertical axis. Providing one inlet and two outlet tube side nozzles allows for simultaneous evaluation of two technologies at the same flow conditions. Measurements of all flow rates and

inlet/outlet temperatures allow us to perform thermal calculations of fouling resistances for two technologies at the same time.

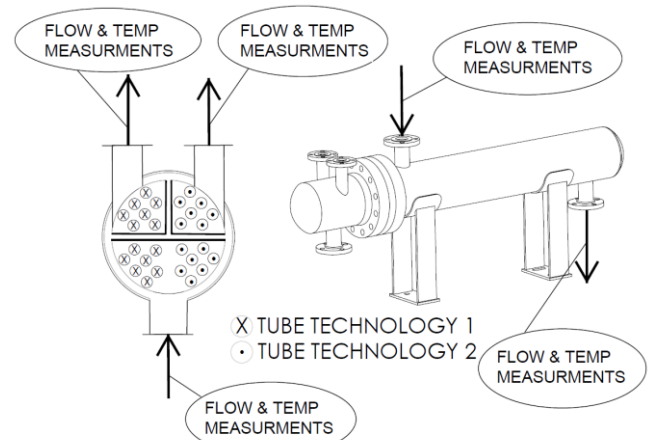


Figure 10. Experimental heat exchanger design to study simultaneously two different heat transfer surface technologies.

In addition to evaluating various coating technologies, the test heat exchanger design shown in Figure 10 allows for tests of surface enhancement, including dual enhancement (outside and inside of the tube) technologies in a controlled environment. As shown by Provost et. al. (2013) and Esawy et. al. (2009) enhanced heat transfer surface technologies may provide significant fouling mitigation benefits in addition to increasing the heat transfer efficiencies. Similarly, as in the case of coating technologies, enhanced heat transfer surfaces may reduce adherence forces of fouling deposits to the surface.

Chevron's experience indicates that both coatings and enhanced heat transfer surface technologies can be successfully deployed to mitigate fouling in industrial facilities.

## CONCLUSIONS

The studies presented in this paper lead to the following conclusions:

1. There are significant differences in composition of fouling deposits collected from actual heat exchangers and fouling deposits developed in laboratory experiments. These differences may explain why fouling threshold models derived from laboratory tests are often not observed in the industrial environment.
2. Ever changing flow and crude slate composition in the crude preheat train heat exchangers can induce large errors in the predictive fouling models derived from fouling trend data. Simultaneous shell side and tube side fouling poses another challenge for accuracy of these models.
3. Simplified experiments that focus on evaluating coatings and heat transfer surface enhancements accelerate development and deployment of fouling mitigation technologies.

## NOMENCLATURE

A	Heat transfer surface area, m <sup>2</sup>
API	American Petroleum Institute
ASME	American Society of Mechanical Engineers
ASTM	American Society for Testing and Materials
DAC	Diamond Anvil Cell
ELSD	Evaporative Light Scattering Detector
FTIR	Fourier Transform Infrared Spectroscopy
HTRI	Heat Transfer Research, Inc.
LVGO	Light Vacuum Gas Oil
MTD	Mean Temperature Difference, °C
Q	Heat duty, W
R <sub>f</sub>	Fouling heat transfer resistance, m <sup>2</sup> -K/W
U <sub>clean</sub>	Overall heat transfer coefficient at clean conditions, W/m <sup>2</sup> -K
U <sub>observed</sub>	Overall heat transfer coefficient calculated based heat balance from field data, W/m <sup>2</sup> -K
XRD	X-ray Diffraction

## REFERENCES

- American Society for Testing and Materials., 2005, Standard test method for determination of asphaltenes (heptane insolubles) in crude petroleum and petroleum products – IP143/01 ASTM D6560.
- Bennett, C.A., Kistler, R.S., Nangia, K., Al-Ghawas, W., Al-Hajji, N., and Al-Jemaz, A., 2009. Observation of an Isokinetic Temperature for High-Temperature Crude Oil Fouling. *Heat Transfer Engineering*, Vol. 30, pp. 794–804.
- Bennett, C.A., 2012, A Theory Describing Asphaltene Adhesion Fouling Inside Heat Exchanger Tubes, *Heat Transfer Engineering*, Vol. 33, pp. 1246–1250.
- Bennett, C.A., 2016, A Theory Describing Sedimentation Particulate Fouling Thresholds Inside Heat Exchanger Tubes, *Heat Transfer Engineering*, Vol. 37, pp. 468-474.
- Bennett, C.A. and Hohmann R.P., 2017, Methods for Calculating Shear Stress at the Wall for Single-Phase Flow in Tubular, Annular, Plate, and Shell-Side Heat Exchanger Geometries, *Heat Transfer Engineering*, Vol. 38, pp 829-840.
- Ebert, W., and Panchal, B., 1996, Analysis of Exxon crude-oil-slip stream coking data, *Fouling Mitigation of Industrial Heat-Exchanger Equipment*, eds. C.B. Panchal, T.R. Bott, E.F.C. Somerscales, and S. Toyama, 451–460, Begell House, NY, USA.
- Esawy, M., Malayeri, M.R., Müller-Steinhagen, H., 2009, Crystallization Fouling of finned tubes during pool boiling: effect of fin density, *Proceedings of Heat Exchanger Fouling and Cleaning Conference, Schlading, Austria*.
- Hirasawa, S., Hijikata, K., Mori, Y., and Nakayama, W., 1980, Effect of surface tension on condensate motion in laminar film condensation, *Int. J. Heat Mass Transfer*, Vol. 23, pp. 1471-1478.
- Jackowski, L, Risse, P., Smith, R., 2017, Impact of nonuniform fouling on operating temperatures in heat exchanger networks, *Heat Transfer Engineering*, Vol 38, pp 753-761.
- Kou, D., Mitra, S. 2003, Extraction of Semivolatile Organic Compounds from Solid Matrices in *Sample Preparation Techniques in Analytical Chemistry*, ed. S. Mitra John Wiley & Sons, Inc., U.S.A., 2003.
- Lopez-Linares, F.; Carbognani, L., Hassan, A., Pereira-Almao, P., Rogel, E., Ovalles, C., Pradhan, A., Zintsmaster, J., 2011, Adsorption of Athabasca Vacuum Residues and Their Visbroken Products over Macroporous Solids: Influence of Their Molecular Characteristics, *Energy and Fuels*, 25 (9), 4049–4054.
- Polley, G.T., 2010, review of the development of models for the prediction of fouling rates in exchangers heating crude oil, *Proceedings 11<sup>th</sup> Annual International Conference on Petroleum Phase Behavior and Fouling, 13-17, Jersey City*.
- Provost, J., El-Hajal, J., Lang, T., 2013, Field tests on heat exchangers equipped with dual enhanced tubes in a quench water application, *Proceedings of Heat Exchanger Fouling and Cleaning Conference, Budapest, Hungary*.
- Pugh, S.J., Ishiyama, E.M., 2015, SmartPM for effective management of crude oil refinery preheat trains and other networks subject to fouling, *American Fuel & Petrochemical Manufacturers Conference, AM-15-62*.
- Rogel, E., Ovalles, C., Moir, M., 2010, Asphaltene Stability in Crude Oils and Petroleum Materials by Solubility Profile Analysis, *Energy and Fuels* 24 (8), 4369-4374.
- Rogel, E., Ovalles, C., Pradhan, A., Leung, P., Chen, N., 2013, Sediment Formation in Residue Hydroconversion Processes and Its Correlation to Asphaltene Behavior, *Energy and Fuels* 27 (11), 6587-6593.
- Rogel, E., Ovalles, C., Moir, M., 2014, Asphaltene Solubility and Fouling ACS National Meeting Book of Abstracts, American Chemical Society - 248<sup>th</sup> ACS National Meeting & Exposition, San Francisco.
- Rogel, E., Ovalles, C., Moir, M., Vien, J.; Morazan, H., 2015, Solubility Characterization of Asphaltene Deposits, *SPE International Symposium on Oilfield Chemistry*, The Woodlands, Texas, USA, SPE -173757.
- Smith, A., 2013, Analysis of fouling rate and propensity for eight crude oil samples in annular test section. *Proceedings of Heat Exchanger Fouling and Cleaning Conference, Budapest, Hungary*.
- Van Nostrand, W. L. Jr., Leach, S. H., Haluska J. L., Economic penalties associated with the fouling of refinery equipment, in *Fouling in Heat Transfer Equipment*, eds. E. F. C. Somerscales and J.G. Knudsen, McGraw-Hill, New York, NY, pp 619-643, 1981
- Wilson, D.I., Ishiyama E.M., Polley G.T., 2015, Twenty years of Ebert and Panchal – what next? *Proceedings of Heat Exchanger Fouling and Cleaning Conference, Enfield (Dublin), Ireland*.